Journal of Biomolecular Structure and Dynamics

ISSN: (Print) (Online) Journal homepage: https://www.tandfonline.com/loi/tbsd20

Exploration of efficacy, cellular responses, and safety profile of novel 9-(3-Pyridyl) noscapine derivatives as promising anticancer candidates

Shruti Gamya Dash, Srinivas Kantevari & Pradeep Kumar Naik

To cite this article: Shruti Gamya Dash, Srinivas Kantevari & Pradeep Kumar Naik (28 Oct 2023): Exploration of efficacy, cellular responses, and safety profile of novel 9-(3-Pyridyl) noscapine derivatives as promising anticancer candidates, Journal of Biomolecular Structure and Dynamics, DOI: 10.1080/07391102.2023.2275177

To link to this article: https://doi.org/10.1080/07391102.2023.2275177

Published online: 28 Oct 2023.

JOURNAL OF BIOMOLECULAR STRUCTURE AND DYNAMICS
https://doi.org/10.1080/07391102.2023.2275177

Taylor & Francis
Taylor & Francis Group

Exploration of efficacy, cellular responses, and safety profile of novel 9-(3-Pyridyl) noscapine derivatives as promising anticancer candidates

Shruti Gamya Dash[a], Srinivas Kantevari[b] and Pradeep Kumar Naik[a]

[a]Centre of Excellence in Natural Products and Therapeutics, Department of Biotechnology and Bioinformatics, Sambalpur University, Sambalpur, India; [b]Fluoro and agrochemicals Division, CSIR-Indian Institute of Chemical Technology, Hyderabad, India

Communicated by Ramaswamy H. Sarma

ABSTRACT

This study presented a novel derivative of the antitussive compound noscapine, named 9-3-Pyridyl noscapine (PYNos), to enhance its anticancer potential. Through in silico investigations, PYNos exhibited strong interactions with microtubules, inhibiting cancer cell proliferation both alone and in combination with docetaxel. Docking scores highlighted the affinity of PYNos −5.67 kcal/mol and docetaxel −4.94 kcal/mol to microtubules. When docked with tubulin-DOX co-complex, PYNos displayed a synergistic score of −8.99 kcal/mol. MTT assays on MCF-7 breast cancer cells showed PYNos IC50 values of 11.0 μM (48 h) and 8.4 μM (72 h), while docetaxel had three orders of magnitude lower IC50 values: 0.028 μM (48 h) and 0.015 μM (72 h). Combining PYNos (25 μM) and docetaxel (0.01 μM) reduced proliferation by 50% at both time points. Isobologram analysis confirmed strong antiproliferative synergy (sum FIC <1) at 48 and 72 h. Our comprehensive evaluation encompassing apoptosis and cell cycle arrest patterns further validated the synergistic advantages of this combination. In a xenograft mice model using MCF-7 cells, the PYNos-docetaxel co-treatment resulted in significant tumor regression, showcasing promising induction of apoptosis while mitigating docetaxel-associated toxicity. In summary, our findings underscore the substantial microtubule interactions facilitated by 9-3-Pyridyl noscapine, revealing its synergistic potential with docetaxel and establishing a solid foundation for advancing cancer therapeutic strategies.

ARTICLE HISTORY
Received 31 January 2023
Accepted 29 September 2023

KEYWORDS
9-(3-Pyridyl) noscapine (PYNos); combination drug therapy; breast cancer; cell proliferation; toxicity analysis

Introduction

Breast cancer treatment options for both locally advanced and metastatic stages encompass medications that target microtubules, such as taxanes (e.g. taxol), vincas, estramustine, halaven, and ixempra. However, the utilization of these drugs has been hindered by considerable adverse effects, including leukocytopenia, diarrhea, alopecia, and peripheral neuropathies, which have led to suboptimal treatment outcomes (Kavanagh & Kudelka, 1993; Rowinsky & Donehower, 1991). This has spurred an ongoing quest to develop innovative mitotic inhibitors with reduced side effects and improved administration convenience. Furthermore, docetaxel, belonging to the taxane class of microtubule-targeting drugs, has demonstrated pronounced efficacy in inhibiting cancer cell proliferation by hindering microtubule dynamics.

Setting itself apart from the current chemotherapeutic agents like taxanes and vincas, noscapine and its derivatives offer a distinctive mechanism. They maintain the structural integrity of microtubule clusters while notably decelerating their dynamic behavior to activate mitotic checkpoints (Ye et al., 1998). Extensive *in vitro* studies, focused on specific microtubules with polymerizing tendencies, along with the monitoring of steady growth at the positive ends, have demonstrated that noscapine primarily influences microtubule dynamics by extending the time microtubules spend in a less active state, as opposed to inducing vigorous depolymerization and repolymerization (Dash & Naik, 2022; Zhou et al., 2003). Encouragingly, both *in vitro* experiments and studies involving mouse xenografts have underscored the effectiveness of noscapine and its synthetic analogs in preventing cancer across diverse tissue origins (Ke et al., 2000; Ye et al., 1998). The noteworthy oral bioavailability of noscapine provides significant backing to its clinical potential as a promising novel chemotherapeutic agent (Aneja et al., 2007; Dahlström et al., 1982), positioning it as a prospective avenue for anticancer treatment with minimal undesirable effects.

Delving into our systematic approach of scaffold structure modification, we have methodically designed and synthesized a range of derivatives (Dash et al., 2023). Prior investigations have illuminated that these compounds exhibit a heightened affinity for tubulin without disrupting the equilibrium between tubulin monomers and polymers. Furthermore, these derivatives have demonstrated the capacity to hinder cell proliferation and induce G2/M cell cycle arrest across a diverse spectrum of human cancer cells (Mahaddalkar et al., 2017; Manchukonda et al., 2013, 2014; Naik et al., 2011; Santoshi et al., 2015). However, despite the development of multiple generations of noscapine derivatives, achieving complete cancer remission has remained elusive. We

CONTACT Pradeep Kumar Naik pknaik1973@gmail.com Centre of Excellence in Natural Products and Therapeutics, Department of Biotechnology and Bioinformatics, Sambalpur University, Jyoti Vihar, Burla, Sambalpur-768 019, Odisha, India.

introduce a novel derivative of noscapine, namely 9-(3-Pyridyl) noscapine (PYNos), and explore its potential when combined with docetaxel (DOX) in the context of anticancer activity.

In summary, the landscape of breast cancer treatment employing microtubule-targeting drugs has been influenced by notable side effects, sparking the search for more effective and better-tolerated alternatives. Noscapine and its derivatives present a unique avenue by preserving microtubule structural integrity while slowing their dynamics. Through meticulous modification of the noscapine molecular scaffold, a variety of derivatives have been crafted, displaying enhanced tubulin affinity, growth inhibition, and cell cycle arrest properties. This study introduces a novel derivative, PYNos, and investigates its synergy with docetaxel for potential anticancer effects.

Materials and methods

Protein preparation

In this phase, we initiated the protein preparation by sourcing the crystal structure of the amino noscapine-tubulin complex (PDB ID: 6Y6D) with a resolution of 2.20 Å (Oliva et al., 2020) from the Protein Data Bank (PDB). Through a meticulous manual examination and refinement of the structure, we obtained a complex comprising both the 'α' and 'β' chains of the protein. Our approach to protein preparation was executed systematically, incorporating the following steps to ensure the integrity of the structure. Firstly, any absent hydrogen atoms were added to the complex. Subsequently, we undertook a multi-step protein preparation process utilizing the Schrodinger software's protein preparation wizard. As a part of this process, water molecules present in the complex were excluded.

To maintain the stability and balance of the structure, side chains that did not play a role in the binding cavity and lacked participation in salt bridges were neutralized. To further refine the energy state of the obtained complex, we employed the OPLS 2005 force field coupled with the PRCG (Polak & Ribiere, 1969) algorithm. This strategic combination facilitated the reduction of energy within the complex, ultimately enhancing its overall stability and suitability for subsequent analyses. Protein preparation strategy involved a meticulous series of steps to optimize the structure's quality. This approach not only ensured the presence of critical components but also optimized the energy balance, thus establishing a solid foundation for our subsequent investigations.

Ligand refinement

Crystal structure of PYNos and DOX was initially created in ChemDraw and then imported to Maestro (Schrodinger) for subsequent refinement. Energy minimization was carried out using Schrodinger's macro model, employing the PRCG algorithm (Polak & Ribiere, 1969) in conjunction with the OPLS 2005 force field. Further refinement involved geometric optimization through Jaguar (Schrodinger) utilizing the B3LYP method (Becke, 1993; Binkley et al., 1980; Gordon et al., 1982; Lee et al., 1988). The generation of distinct molecular isoforms was accomplished using Ligprep (Schrodinger).

Analysis of PYNos through molecular modelling as a tubulin-binding agent and its interaction with docetaxel

Employing the Glide XP (Extra Precision) docking algorithm by Schrödinger (Halgren et al., 2004), both PYNos and DOX were subjected to docking with the αβ-tubulin dimer. The docking process positioned them at the centroid of their respective binding sites. For the molecular dynamics (MD) simulation, the Amber 16 simulation package was employed. The simulation encompassed four scenarios: (a) PYNos docked with tubulin, (b) DOX docked with tubulin, (c) the combined presence of PYNos and DOX with tubulin, and (d) tubulin alone. Prior to the simulation, the protein and ligand structures were optimized. Missing hydrogen atoms were added, and the respective parameters for molecules were allocated using the FF14SB and GAFF force fields, as outlined by Jordan and Wilson (2004). The methodologies outlined in earlier work (Dash, Kantevari, et al., 2021) were followed for these procedures.

Biology

Cell lines and chemicals

The lead compounds noscapine and docetaxel were provided by Sigma. To synthesize the potent derivatives of PYNos, chemical synthesis was employed followed by refinement and purification using HPLC. Additional chemicals and culture media essential for cell culture were procured from Mediatech and Cellgro. The MCF-7 breast cancer cell line was obtained from NCCS in Pune, Maharashtra, India. For preparing a stock solution (100 μM) of PYNos, dimethyl sulfoxide (DMSO) was utilized and stored at 4 °C. The cells were cultivated in Dulbecco's modified Eagle medium (DMEM), contained antibiotics and 10% fetal bovine serum (FBS), and were kept at 37 °C with 5% CO_2 and 95% humidity.

In vitro cytotoxicity assay using MCF-7

In this experiment, we conducted an *in vitro* cytotoxicity assay using the MCF-7 human breast cancer cell line to assess the antiproliferation activity of test compounds. The cells were cultured in 96-well plates at a density of 3×10^3 cells per well. The test compounds used were PYNos and DOX. For the assessment of PYNos, the cells were treated with various concentrations: 0, 5, 10, 25, and 50 μM. Similarly, for DOX, the cells were treated with varying concentrations: 0 μM, 0.001 μM, 0.01 μM, 0.1 μM, and 1 μM. To study the combined effect of PYNos and DOX, the cells were treated with different concentrations: 5 μM PYNos + 1 μM DOX, 10 μM PYNos + 0.1 μM DOX, 25 μM PYNos + 0.01 μM DOX, and 50 μM PYNos + 0.001 μM DOX. These treatments were administered directly to the medium after allowing the cells to adhere for 12 h. Cell viability was assessed through the implementation of the 3-(4,5-dimethylthiazol-2-yl)-2,5-ditetrazolium bromide (MTT) assay. This assay allowed us to assess cell viability after a specific duration of time. (Dash et al., 2020, 2021, 2021).

Isobologram analysis was used to determine the drug interaction

Isobologram analysis, a more traditional method, is used to evaluate the additive, synergistic, or antagonistic effects of the compounds PYNos and DOX. This approach has been discovered and mathematically verified effectively. Since the combination of PYNos and DOX has been utilized in a variable dose ratio, a standardized isobologram for the two drugs at their IC_{50} was automatically created by CompuSyn software (ComboSyn Inc., Paramus, NJ) (Dash et al., 2021). It was accomplished using Chou-Talalay's combination index (CI) method. The positioning of combined data points on the normalized isobologram indicates an additive effect (when points align with the hypotenuse), synergism (if points cluster in the lower-left quadrant), or antagonism (if points cluster in the upper-right quadrant). Logit regression analysis was used to determine the IC50. In order to interpret the fractional inhibitory concentration (FIC), the formula shown below was utilized:

$$FIC = \frac{Conc.of\ drug\ in\ combination\ to\ produce\ IC_{50}}{Conc.\ of\ drug\ alone\ require\ to\ produce\ IC_{50}}$$

The drug-drug interaction was categorized based on the cumulative FIC value for every compound as calculated using the formula below.

$$Sum\ FIC = \frac{IC_{50}\ of\ drug\ A\ in\ combination}{IC_{50}\ of\ drug\ A\ alone} + \frac{IC_{50}\ drug\ B\ in\ combination}{IC_{50}\ of\ drug\ B\ alone}$$

Cell cycle analysis

We explored the influence of PYNos and DOX treatments on cell cycle regulation in MCF-7 cells, aiming to understand their effects on both inhibiting cell proliferation and inducing apoptosis. To achieve this, we employed PYNos and DOX as interventions to impede the progression of the cell cycle. Assessment of cell cycle alterations was conducted using a methodology detailed in the work of Dash et al. (2021). We employed a flow cytometer, specifically the FACS Calibur system, to perform cell cycle analysis. This approach allowed us to quantify the distribution of cells across distinct phases of the cell cycle, providing insights into potential mechanisms by which PYNos and DOX influence cell cycle dynamics.

Apoptosis assay by flow cytometry

MCF-7 cells at a density of 5×10^4 were cultured in 12-well culture plates. The cells were treated with three different conditions: PYNos (20 μM), DOX (0.1 μM), or a combination of both (25 μM PYNos + 0.01 μM DOX). The cells were incubated for 24 h, following the established protocol outlined in a previous study by Dash et al. (2021). The primary focus of this study was to observe the movement of phosphatidylserine (PS) from the inner to the outer side of the plasma membrane, a common hallmark of apoptosis. This process was assessed using flow cytometry, specifically the BD FACS Calibur instrument, in accordance with the manufacturer's provided instructions.

Tryptophan-quenching assay

In the tryptophan-quenching assay, tubulin at a concentration of 2 μM was obtained through the extraction and isolation process from goat brain tissue. This isolation involved multiple rounds of GTP-induced assembly and temperature-dependent disassembly. The tubulin samples were then subjected to incubation with a PEM buffer, PYNos at 20 μM, and DOX at 0.1 μM. Additionally, combinations of these compounds were tested, specifically a combination of DOX at 0.01 μM and PYNos at 25 μM. To assess the interactions and effects of these compounds on tubulin's tryptophan fluorescence, spectrofluorometric titrations were performed. The instrument employed for these measurements was the FlouroMax® 4 spectrofluorometer, manufactured by Horiba Scientific located in Edison, NJ. The Fluor Essence 3.5 software, as detailed in Dash et al. (2020), was utilized to control and acquire the spectrofluorometric data.

ANS binding assay

The effects of concentrations of PYNos and DOX, both individually and in combination, on tubulin were investigated. Tubulin (2 μM) was subjected to incubation with PYNos concentrations (20 μM), along with a consistent DOX concentration (0.1 μM), and with reduced DOX concentrations (0.01 μM) in conjunction with either 25 μM of PYNos. Subsequently, the samples were treated with ANS (50 μM) and kept in the dark at 25 °C for 15 min. This process follows established methods outlined in previous studies (Chougule et al., 2011; Mahaddalkar et al., 2017). The goal of this procedure was to assess potential changes in tubulin structure and behavior in response to the different compound concentrations.

Breast cancer xenograft models

The experimental procedures concerning animal subjects underwent ethical evaluation and received approval from the Institutional Animal Ethics Committee at the National Institute of Pharmaceutical Education and Research (NIPER) in Hyderabad. The approval reference number was 1548/PO/Re/2011/CPCSEA. The procedures adhered to the established standards set by the Indian government for animal experimentation. Female BALB/c immunodeficient nude mice, aged 8–10 weeks, were housed in sterilized cages. To initiate the experiments, a suspension of 1×10^6 MCF-7 cells in 0.2 mL of phosphate-buffered saline (PBS) was subcutaneously implanted in the anterior flank of the mice. Once the tumors became visible, which typically took 7–10 days, administration of the test drugs began. The mice were categorized into four distinct groups:

1. Group 1 (Control): Comprising five animals, this group was subjected to a daily oral dosing of a vehicle solution—acidified water at pH 4.0.

Table 1. The results of the docking score (Glide XPscore) and the exposure energy parameters.

Ligands	Glide XP_{score} (kcal/mol)	Glide E_{vdw} (kcal/mol)	Glide E_{coul} (kcal/mol)	Glide Energy (kcal/mol)
PYNos	−5.67	−28.76	−9.01	−37.78
DOX	−4.94	−37.80	−8.24	−38.35
PYNos docked with Tubulin_DOX complex	−8.99	−40.99	−10.19	−51.19
DOX docked with PYNos complex	−5.88	−38.26	−11.96	−50.22

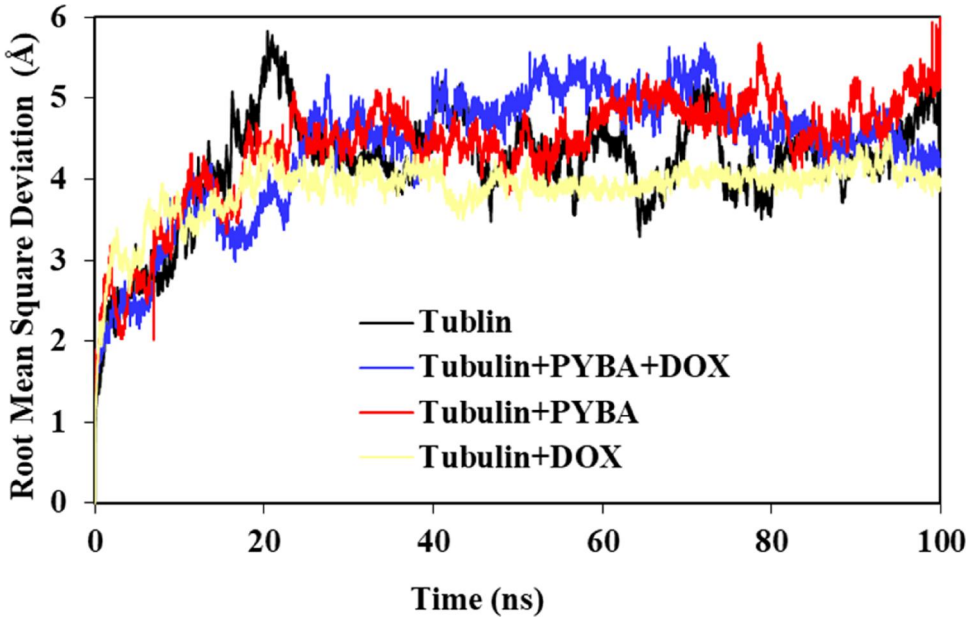

Figure 1. MD simulation at 100 ns were analysed using the root mean square deviations (Cα-RMSD).

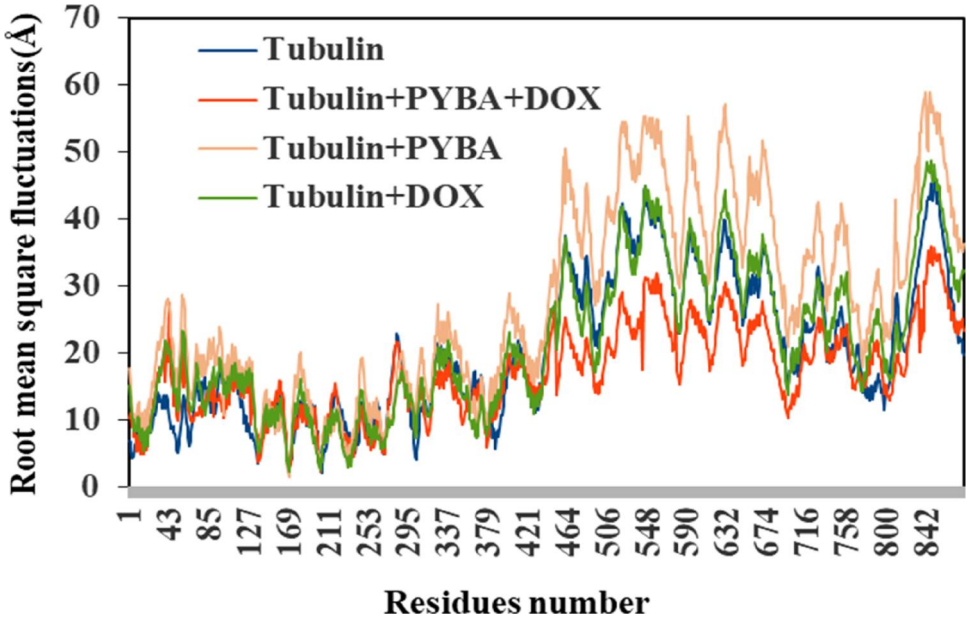

Figure 2. The root mean square fluctuation (RMSF) of the docked ligands' tubulin residues in the bound and unbound tubulin heterodimer shape.

2. Group 2: In this group, five animals were administered PYNos at a dose of 150 mg/kg/day.
3. Group 3: five animals in this group were treated with DOX at a dose of 1.5 mg/kg/week, administered intravenously.
4. Group 4: This group comprised five animals that received a combined treatment of PYNos and DOX. The doses were PYNos at 300 mg/kg/day and DOX at 1.0 mg/kg/week, both administered intravenously. This strategy was devised to attenuate the dosage of docetaxel while concurrently augmenting the PYNos dosage, thereby mitigating concentration-dependent docetaxel-associated toxicities.

Tumor volume measurements were conducted on alternate days using vernier calipers in three transverse orientations. The tumor volume was calculated using the formula $V = \pi/6 \times (\text{length} \times \text{breadth} \times \text{height})$, as described by

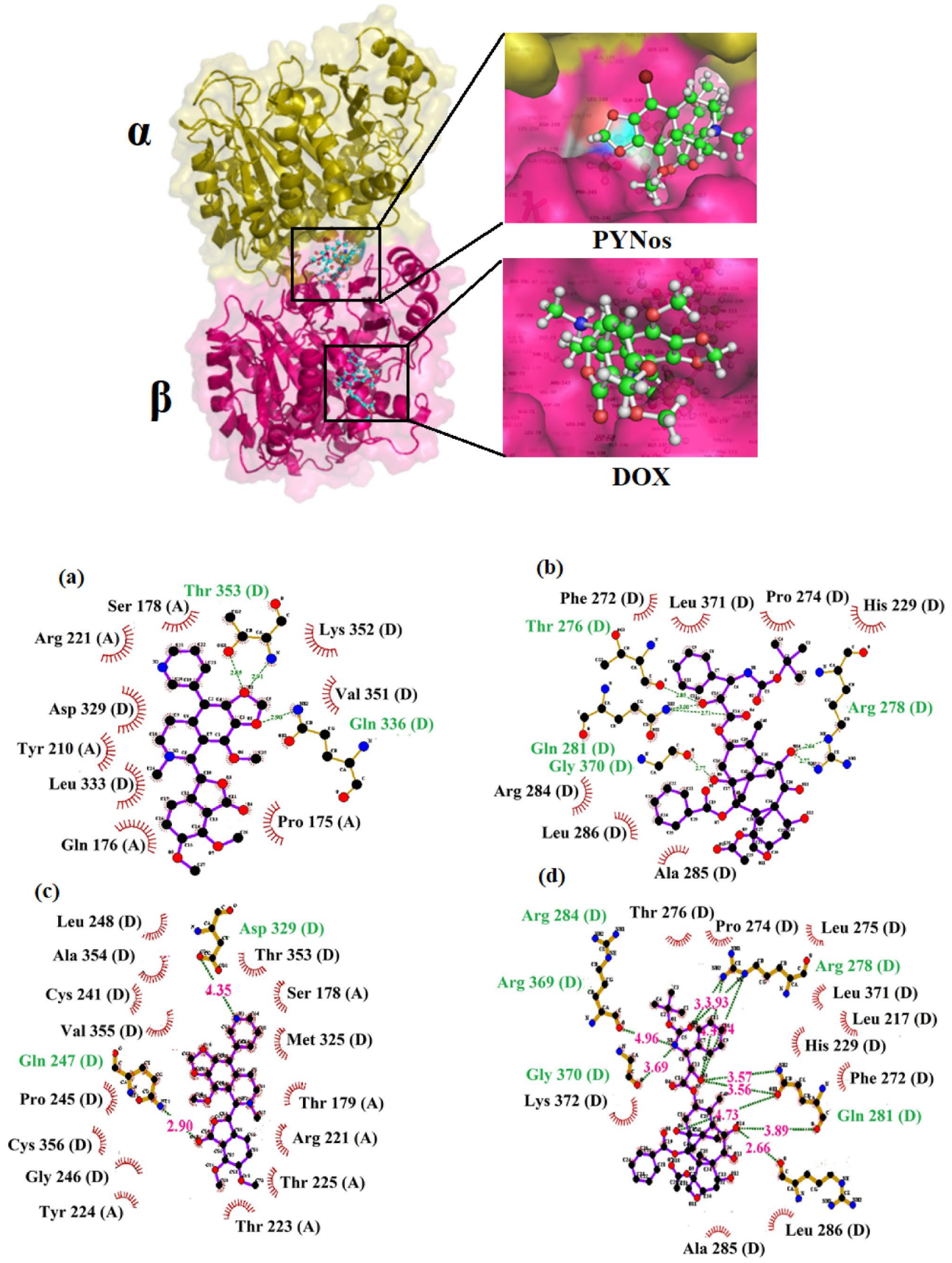

Figure 3. Overview of the binding mode of both the ligands and their ligplot analysis. The ligplot analysis showing the binding mode of (a) PYNos in single and (b) DOX in single. The binding site residues involved in the interaction of PYNos are slightly different in combination with DOX. Similarly, the ligplot analysis showing the binding mode of (c) PYNos when it is docked into the co-complex of tubulin and DOX (d) DOX when it is docked into the co-complex of tubulin and PYNos. The binding site residues involved in the interaction of DOX are slightly different in combination with PYNos. The hydrogen bonds formed (if any) are represented as dotted lines.

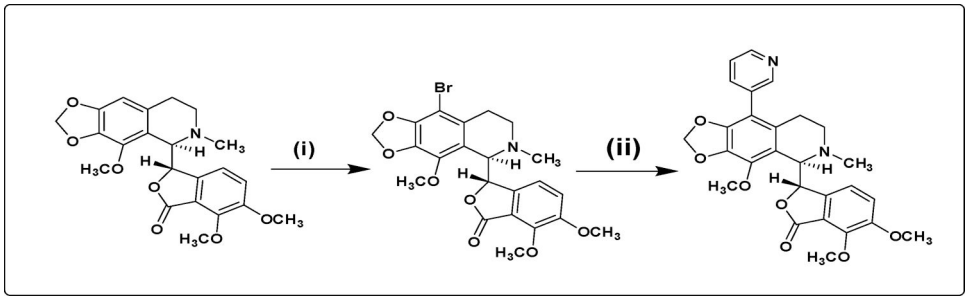

Scheme 1. Synthesis of 9-(3-Pyridyl) noscapine (PYNos): reaction conditions. (i) 48% HBr, Br_2-water, rt, 2h, 90% (ii) 3-Pyridyl boronic acid, $Pd(TPP)_4$, $NaHCO_3$, EtOH/Toluene, 120 °C, 48 h, 62%.

Tomayko and Reynolds in 1989. At the end of the experimental period, on day 30, the mice in Group 1 (control) were euthanized due to extensive tumor growth. This time point served as a terminal endpoint for the control group. This endpoint was chosen to compare tumor growth among the untreated, PYNos-treated, and DOX-treated mice.

Histologic and hematologic analyses

On the 40th day of the experiment, tumor-bearing mice that had undergone treatment with PYNos and DOX, both separately and in combination, along with untreated tumor-bearing mice, were anesthetized using an overdose of 3.5% chloral hydrate (0.2 mL). Hematological samples were obtained directly from the heart and analyzed using a CBC analyzer from CDC Technologies located in Oxford, CT. Subsequently, specific sections of interest and the tumors themselves were extracted. To prepare for histological examination, the animals were perfused with a solution containing 3% paraformaldehyde and 2% glutaraldehyde in phosphate-buffered saline (PBS) at a pH of 7.4. The extracted sections and tumors were then embedded in paraffin. Tumor viability was assessed by examining sections of tumors stained with hematoxylin and eosin. This approach allowed for a comprehensive evaluation of the effects of the different treatments on tumor-bearing mice, including those adminstred with PYNos and DOX either separately or in combination, as well as untreated mice with tumors.

Results and discussion

Molecular modeling

There is a strong probability that both noscapinoids and docetaxel will have an additive impact because they are both known to bind to tubulin at distinct binding sites (Dash et al., 2021; Naik et al., 2011). To evaluate the predicted binding affinities of ligands separately and in combo, we molecularly docked them twice to their binding pockets. DOX and PYNos docked separately to their appropriate binding sites in the first cycle, with docking scores of −5.67 kcal/mol and −4.94 kcal/mol, accordingly (Table 1). The tubulin-PYNos co-complex was taken in the second cycle and DOX was docked at its binding site to evaluate the change in DOX binding affinity in single and combination modalities with PYNos. Correspondingly, the DOX-tubulin co-complex was chosen and PYNos was docked to its binding site to evaluate the difference in binding affinity of PYNos in the single and in a combined regimen with DOX.

The docking score of PYNos (−5.67 kcal/mol) was decreased to −8.99 kcal/mol due to the docking of DOX. Similarly, the docking score of DOX (−4.94 kcal/mol) was further decreased to −5.88 kcal/mol when PYNos was docked. Compared to single binding, the significant reduction in the docking score when both the ligands were bound together may be due to the alteration in tubulin conformation (Najmanovich et al., 2000).

MD simulation

Tubulin-PYNos and Tub-DOX complexes, as well as Tub-DOX + PYNos, were used in MD simulations of 100 ns to study the binding of both PYNos and DOX. In order to track the stability of the process, root mean square deviations (RMSD) of C α-atoms were calculated for each frame (Figure 1).

Residue numbers were displayed against the RMSF values depending on the 100 ns trajectory (Figure 2). More versatility seems to be demonstrated by residues with significantly larger RMSF. Both PYNos and DOX were well positioned within the binding cavity. PYNos demonstrated effective docking at the α and β-tubulin interface, whereas DOX exhibited a binding preference primarily towards β-tubulin (Figure 3(a,b)).

Chemistry

Synthesizing various noscapine derivatives poses a challenge due to the inherent instability of the C–C bond within the isoquinoline and isobenzofuranone ring elements, rendering them susceptible to strong acids and bases. Additionally, achieving a standardized approach for fusing PYNos without disrupting this responsive C-C bond remains complex. In this context, the reaction between 9-bromonoscapine and 3-pyridyl boronic acid was executed under nitrogen using Pd (PPh3)4 (0.049 μmol) and sodium bicarbonate (0.82 μmol). Thorough characterization of both 9-Br-Noscapine and PYNos was conducted through 1H, 13 C NMR, mass (ESI and HRMS), and IR spectral data (Scheme 1).

Biology

Novel PYNos prevents the growth of MCF-7 cancer cells

The potential of PYNos to inhibit the proliferation of MCF-7 in single-agent and combined regimens with DOX was

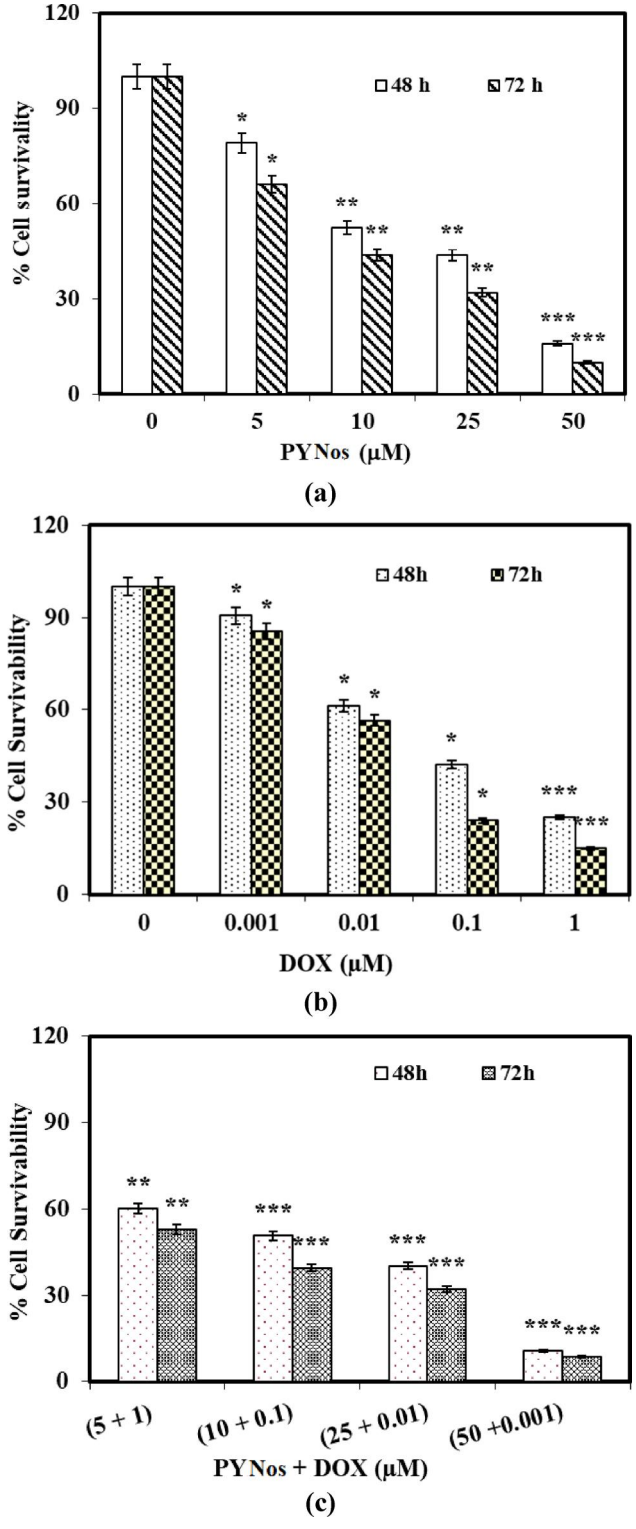

Figure 4. The bar chart depicts the impact of treatment with PYNos and DOX administered individually and in combination on the percentage of cell viability in MCF-7 cancer cells. The results indicate a significant reduction in cell viability following treatment with both PYNos and DOX, either as single agents or in combination. This decrease in cell viability suggests the potential cytotoxic effect of the treatments on MCF-7 cancer cells. The experiments were performed in triplicate, and the data shown are representative of these replicates.

analyzed. Elevated concentrations of PYNos and DOX, whether administered individually or in combined formulations, exhibited heightened anti-proliferative efficacy (Figure 4). PYNos displayed IC50 values of 11.0 μM (48 h) and 8.4 μM

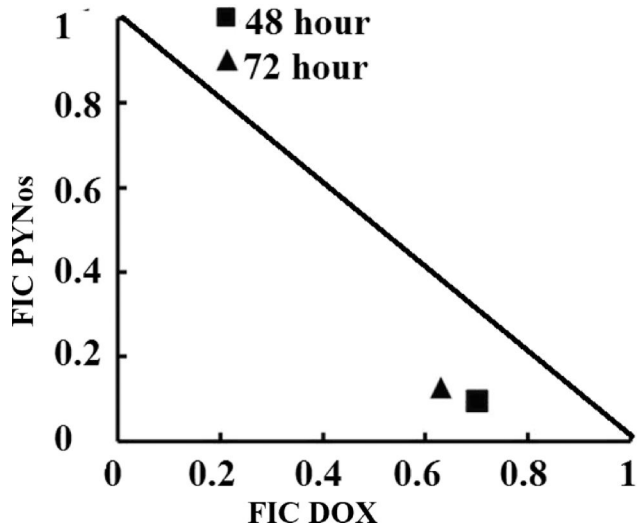

Figure 5. The interactions between PYNos and DOX *in vitro* are shown by isobolograms.

(72 h), while DOX exhibited IC50 values of 0.028 μM (48 h) and 0.015 μM (72 h). After 48 and 72 h of treatment, the combined regimen of PYNos (25 μM) and DOX (0.01 μM) reduced cellular growth by substantially 50% (Figure 4(c)). Findings showed that PYNos and DOX significantly decreased the dosage and time-dependent viability of MCF-7 cells compared to control with treated.

Interaction between the two agents has also been evaluated (Figure 5) using their sum FICs and isobologram representation. The cumulative FICs value was determined to be 0.8 and 0.76 both at 48 and 72 h. The combined regimen displays synergistic antiproliferative efficacy at both 48 and 72 h of exposure, according to the isobologram of PYNos with DOX (sum FIC <1).

Cell cycle analysis

To verify the induction of apoptosis, FACS was used to investigate the effect of PYNos and DOX on the cell cycle profile of MCF-7. The results are shown in Figure 6. A reliable indicator of cell cycle profile and cell death is fluorescently labeled DNA deposition. The G1 stage is represented by the cells with 2 N DNA. In contrast, cells with duplicated 4 N DNA indicate G2/M phases. Cells in the DNA replication process with peaks of 2 N and 4 N reflect the S phase as DNA is being synthesized, whereas less is shown in populations of dying cells that reduce their DNA to different extents. Substantial cell cycle profiling alterations were seen after test substances were administered to MCF-7 cells for 48 h. The FACS data indicates high cell accumulation in the G2/M phase following 48 h of treatment with PYNos (20 μM) and DOX alone (0.1 μM) and in combined regimens (25 μM PYNos + 0.01 μM DOX), relative to untreated cells.

Apoptosis assay

We investigated whether PYNos, alone or in combination with DOX, caused apoptotic cell death in breast cancer cells. The translocation of phosphatidylserine, which is typically on the inner leaflet of the cell membrane, to the outer leaflet

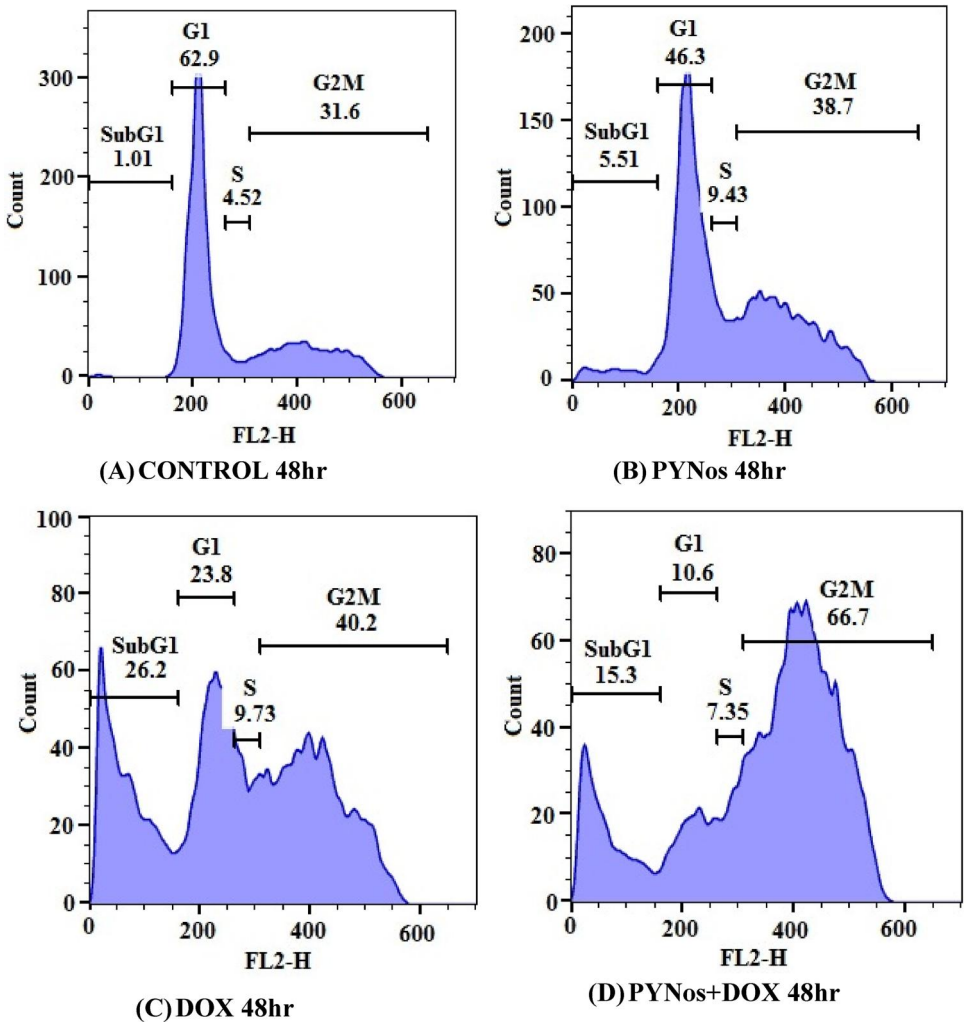

Figure 6. Panels (A) to (D) illustrate the cell cycle distribution of MCF-7 cells in a two-dimensional arrangement after 48 h of treatment with a single regimen of 20 μM of PYNos and 0.1 μM of DOX or a combined regimen of 25 μM of PYNos and 0.01 μM of DOX. The outcomes demonstrate progression through the mitotic cell cycle followed by the appearance of a prominent hypodiploid (Sub-G1) DNA peak, which is a hallmark of apoptosis.

can be detected fluorescently by annexin V binding. The apoptotic mechanism is biochemically linked to changes in the lipid composition of the cell membrane. Apoptotic cells can be measured to a substantial extent using FACS analysis. Figure 7 demonstrates the density plots procured from control and treated MCF-7 cells. As expected, the amount of PYNos (25 μM) + DOX (0.01 μM) treated apoptotic cells was 26.1% (early apoptotic cells) and 19.9% (late apoptotic cells). In contrast, treatment with a single regimen of PYNos (20 μM) leads to 13.0% early apoptotic cells and 8.56% late apoptotic cells and DOX (0.1 μM) leads to 11.0% early apoptotic cells and 3.99% late apoptotic cells. This finding revealed that the possible combined effect of PYNos and DOX would efficiently induce apoptosis in cancer cells and represent a promising potential of reducing DOX toxicity

Tryptophan quenching Assessment

Tubulin's autofluorescence originates from its tryptophan content. The diminishing fluorescence intensity at rising PYNos and DOX concentrations, whether separately or combined, implies their binding to tubulin. Comparable differences in fluorescence intensity were observed as 34.03% (20 μM PYNos), 30.51% (0.1 μM DOX), and 68.72% (combined 0.01 μM DOX and 25 μM PYNos) (Figure 8). In the combined PYNos and DOX treatment, the notable decline in tubulin's fluorescence intensity underscores the concurrent binding of both ligands with tubulin.

PYNos and DOX altered the morphological features of tubulin

PYNos tubulin treatment significantly improved tubulin-ANS fluorescence intensity in a concentration-dependent manner (Figure 9). At 20 μM of PYNos, the fluorescence intensity was found to be improved by 25%, whereas DOX (0.1 μM) was higher than unbound tubulin by 42.9%. Corresponding to this, when PYNos (25 μM) and DOX (0.01 μM) were administered synergistically, the fluorescence intensity of the tubulin-ANS fluorescence increased to 59% suggesting that the structural integrity of tubulin is being gradually compromised.

Antitumor activity

Administred with PYNos (150 mg/kg/day), DOX (1.5 mg/kg/week, i.v), or in combination (PYNos 300 mg/kg/day + DOX

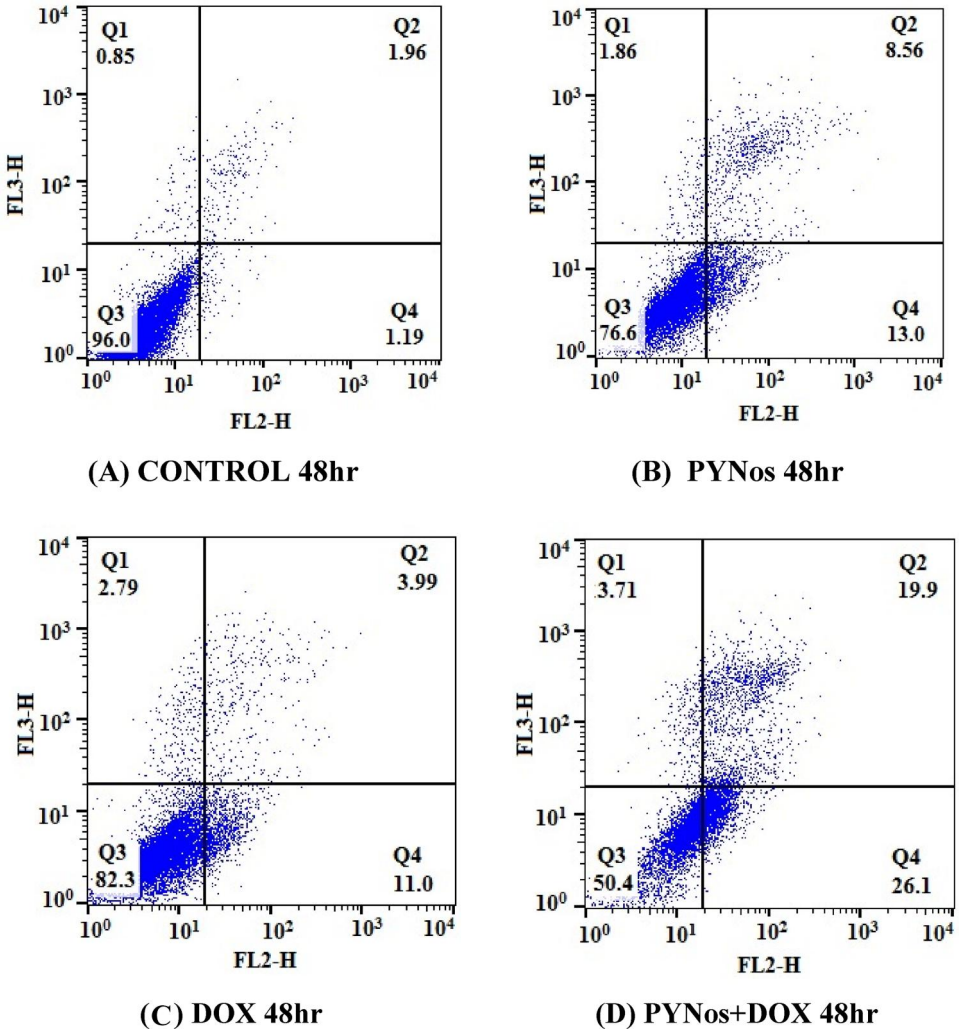

Figure 7. Flow cytometric investigation of the induction of apoptotic cell death by PYNos alone and in combination with DOX.

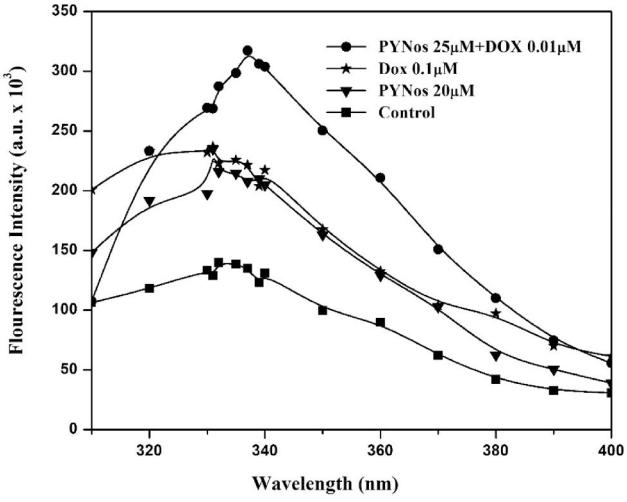

Figure 8. PYNos and DOX, when proposed either individually or in combination, significantly decrease the fluorescence intensity of tubulin and the emission spectra were obtained (320 nm–400 nm). the graph demonstrates the outcomes of three independent observations.

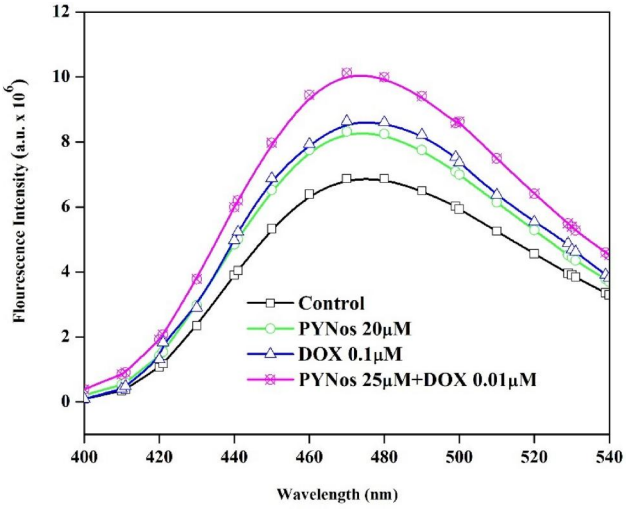

Figure 9. PYNos and DOX, both alone and in combination, increase the fluorescence of the tubulin-ANS protein. Tubulin (2.0 μM) was incubated alone (control), with PYNos (20 μM), DOX (0.1 μM), or in combination (PYNos 25 μM + DOX 0.01 μM). the graph is representative of three independent experiments.

1.0 mg/kg/week, i.v,) significantly reduced tumour volume as compared to control ($p < 0.001$) (Figure 10(A)). By the 40th day post tumor implantation, the tumor volume exhibited reductions to 620 mm^3 through combination treatment, 946 mm^3 with DOX, and 1122 mm^3 with PYNos, compared to the initial 1630 mm^3 in the untreated control group. Solid

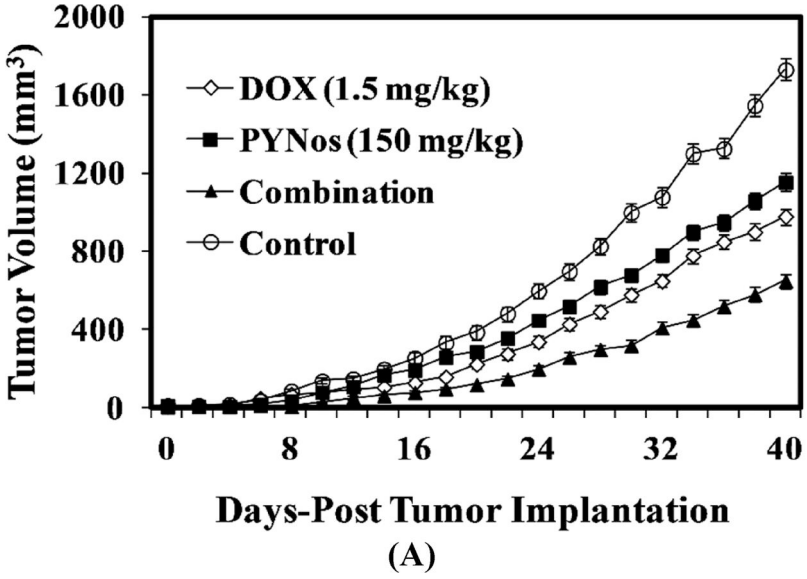

(A)

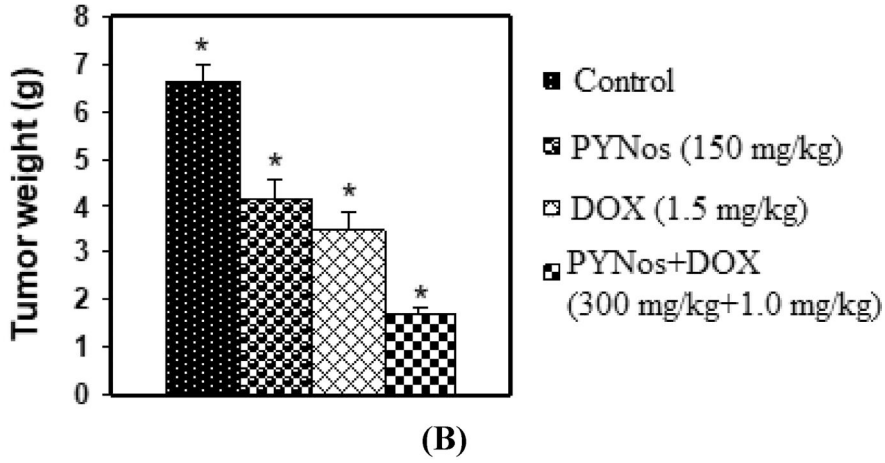

(B)

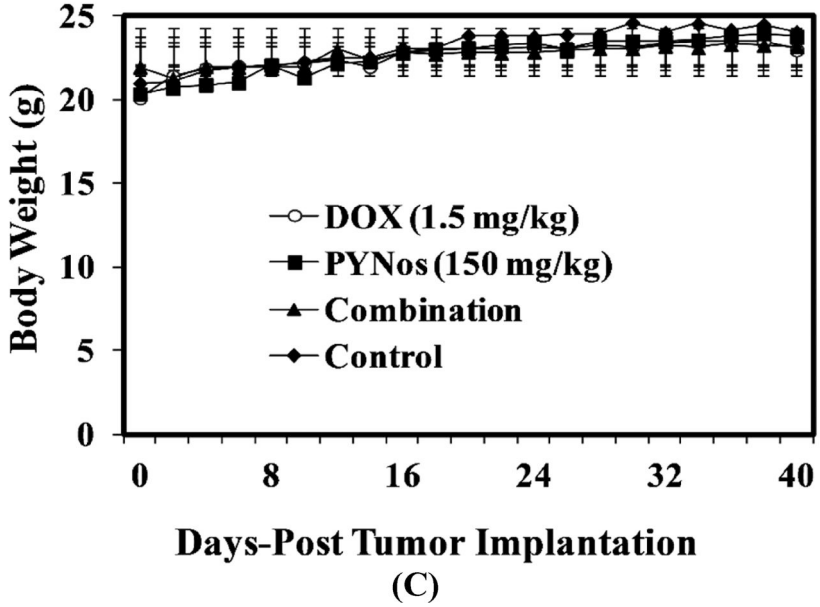

(C)

Figure 10. (A) On a human MCF-7 tumour xenograft model, the development profile of tumour growth kinetics of in-vivo anticancer effect of treatment dosages of PYNos and DOX alone and in combination regimen (tumor volumes, mm3 ± SEM), (B) and body weight measurements after PYNos alone, DOX alone, and in combination regimens. Female nude mice with xenograft MCF-7 tumours underwent various treatments for 30 days starting on day 7 post-tumor implantation. PYNos (150 mg/kg/day), DOX (1.5 mg/kg intravenously), and PYNos 300 mg/kg/day + DOX 1.0 mg/kg/week were administered to the mice. The group under control only received a vehicle. The significant difference in tumour volume between the treatment groups and the control group is statistically significant. $p < 0.01$(**, significantly different from PYNos and DOX single treatments; *, substantially different from untreated controls). This experiment was conducted twice.

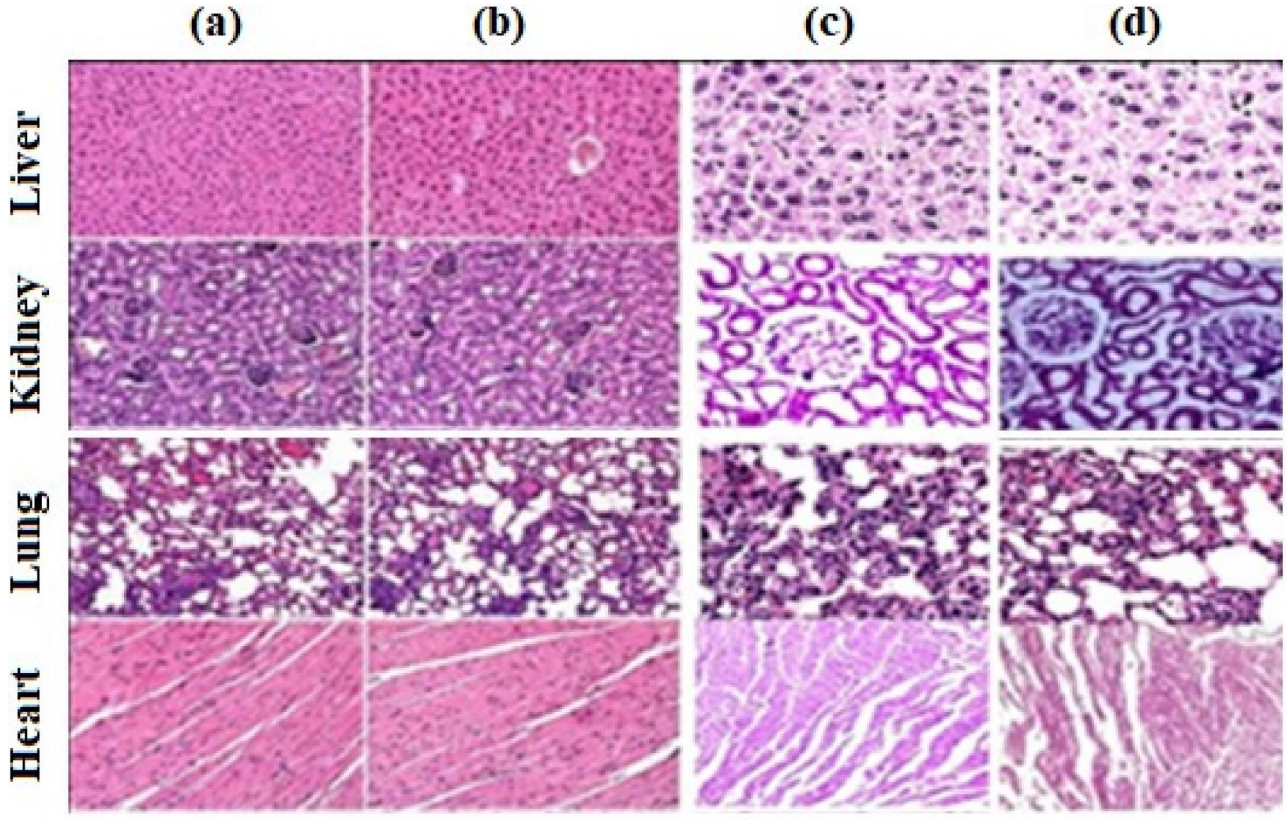

Figure 11. Represent H&E staining of paraffin-embedded 5.0 micron-thick sections of (a)Vehicle, (b) PYNos (150 mg/kg body weight/day), (c) DOX (1.5 mg/kg body weight/ week), (d) (PYNos 300 mg/kg body weight/day + DOX 1.0 mg/kg body weight/week, the heart, lung, kidney and liver at a magnification of 200×.

Table 2. Treated animals with (a) Vehicle, (b) PYNos (150 mg/kg body weight/day), (c) DOX (1.5 mg/kg body weight/ week), (d) (PYNos 300 mg/kg body weight/ day + DOX 1.0 mg/kg body weight/week showed no difference in different blood parameters indicating lack of toxicity.

Parameter	Vehicle	PYNos (150 mg/kg body weight/day)	DOX (1.5 mg/kg body weight/ week)	PYNos (300 mg/kg body weight/day) + DOX (1.0 mg/kg body weight/week)
WBC count (10^3/μL)	3.6 ± 1.5	3.8 ± 1.7	3.9 ± 1.4	3.8 ± 1.2
Monocytes (%)	0.5 ± 0.03	0.4 ± 0.03	0.6 ± 0.02	0.5 ± 0.04
Eosinophils (%)	0.8 ± 0.02	0.7 ± 0.03	0.6 ± 0.04	0.7 ± 0.06
RBC count (10^6/μL)	4.9 ± 0.08	5.2 ± 0.2	5.9 ± 0.3	5.8 ± 0.6
Haemoglobin (g/dL)	14.2 ± 2.6	15.8 ± 1.5	16.2 ± 1.9	14.9 ± 2.1
Hematocrit (%)	42.4 ± 1.8	45.2 ± 1.8	47.2 ± 2.4	44.7 ± 2.7
Mean corpuscular volume (fL)	63.4 ± 1.7	65.5 ± 3.6	68.9 ± 1.6	64.8 ± 3.5
Mean corpuscular hemoglobin (pg/cell)	28.2 ± 1.5	27.8 ± 1.4	30.4 ± 1.5	29.4 ± 1.7
Mean corpuscular hemoglobin concentration (g/dL)	28.4 ± 1.6	32.1 ± 2.3	33.9 ± 1.8	29.7 ± 1.3
Platelet (10^3/μL)	93.5 ± 2.4	99.2 ± 4.6	98.6 ± 5.7	95.7 ± 3.6

tumors in untreated mice ranged in size from 5.6 g to 10.5 g (mean 7.8 ± 2.0 g) in weight. The significant administered groups had only modest palpable tumours and a considerable regression in tumour growth. The average tumor weight with standard error for both control and experimental mice is illustrated in Figure 10(B). In comparison to untreated control mice, PYNos and DOX administered individually and in combination protocols reduced tumor growth found to be significantly ($p < 0.001$). These results demonstrate that when PYNos and DOX are administered together, the tumor size is significantly reduced compared to when PYNos and DOX are administered separately. Additionally, we found no obvious weight reduction following the drug treated as compared with the untreated group mice (Figure 10(C)).

Toxicity analysis

The severe adverse reactions to chemotherapy are one of the biggest challenges in the context of cancer therapy. While tubulin-binding drugs such as vinca alkaloids and taxanes have been received clinical approval, they are known to induce undesirable complications (Rowinsky, 1997). Developing a treatment regimen that is stable and well-tolerated would therefore be essential. In order to determine whether PYNos and DOX had any harmful effects on healthy tissues when used alone or in combination, we looked at the liver, kidney, lung, and heart of tumor-bearing mice. Figure 11 illustrates the hematoxylin and eosin (H&E) staining performed on 5.0-micron thick sections of paraffin-embedded liver, kidney, lung, and heart tissues, captured at a magnification of 200×. Moreover, we identified

no differences in hematological and biochemical parameters between treated and control animals (Table 2).

Discussion

The presented study investigated the potential synergistic effects of the combination of PYNos (a novel noscapinoid derivative) and DOX (docetaxel) that impair the proliferation of MCF-7 breast cancer cells. The research encompassed several key aspects, including molecular modeling, molecular dynamics (MD) simulations, chemical synthesis, biological assays, and toxicity analysis. Molecular modeling and MD simulations were utilized to explore the binding affinities and stability of PYNos and DOX individually and in combination with tubulin, the target protein. The results indicated that both ligands bind to distinct sites on tubulin. Both ligands proved to have a stable affinity with tubulin, as evidenced by the molecular dynamic simulation for 100 ns. As a comparison to their individual treatment regimens, the reduction of proliferative activity was improved dramatically when both treatments were administered simultaneously. The docking scores revealed strong binding affinities, which were further reduced when the ligands were docked together. The combination of PYNos and DOX demonstrated synergistic antiproliferative efficacy, as evidenced by the sum of FICs and isobologram analysis. The treatment with PYNos and DOX, both separately and in combination, led to significant cell cycle profile alterations, with a pronounced impact on the G2/M phase, indicating potential disruption of cell cycle progression. Fluorescence quenching assay and morphological analysis of tubulin indicated that both PYNos and DOX bind to tubulin, affecting its structural integrity. The toxicity analysis indicated that the combination treatment did not induce adverse effects on healthy tissues, as observed in histological and biochemical assessments.

Conclusion

Intensive molecular modeling, cellular and biochemical data analysis, and *in vivo* animal experimental tests have all demonstrated the importance of synergistic effects of the recently discovered noscapine derivative (PYNos) and docetaxel. The overall results of the study collectively suggest that the combination of PYNos and DOX exhibits promising antitumor effects on breast cancer cells. The synergy between these agents was evident in multiple aspects, including antiproliferative effects, apoptosis induction, cell cycle alterations, and tumor growth reduction. Additionally, the combination treatment demonstrated a lack of significant toxicity to healthy tissues. The concurrent utilization of PYNos and DOX has the potential to introduce an innovative approach towards the treatment of breast cancer.

Disclosure statement

The authors declare that they have no conflicts of interest that are relevant to the content of this article. All data generated or analyzed during this study are included in this article.

Funding

Shruti Gamya Dash wishes to acknowledge the award of student research fellowship [DST/INSPIRE/Code No.: IF170022]. We would like to acknowledge the financial support provided by the OHEPEE, Govt. of Odisha through the World Bank. We are grateful to Dr. Manu Lopus and the UM-DAE Centre for Excellence in Basic Sciences for providing extended facilities.

ORCID

Shruti Gamya Dash http://orcid.org/0000-0002-3905-2399
Pradeep Kumar Naik http://orcid.org/0000-0001-7044-2427

References

Aneja, R., Dhiman, N., Idnani, J., Awasthi, A., Arora, S. K., Chandra, R., & Joshi, H. C. (2007). Preclinical pharmacokinetics and bioavailability of noscapine, a tubulin-binding anticancer agent. *Cancer Chemotherapy and Pharmacology*, *60*(6), 831–839. https://doi.org/10.1007/s00280-007-0430-y

Becke, A. D. (1993). A new mixing of Hartree-Fock and local density-functional theories. *The Journal of Chemical Physics*, *98*(2), 1372–1377. https://doi.org/10.1063/1.464304

Binkley, J. S., Pople, J. A., & Hehre, W. J. (1980). Self-consistent molecular orbital methods. 21. Small split-valence basis sets for first-row elements. *Journal of the American Chemical Society*, *102*(3), 939–947. https://doi.org/10.1021/ja00374a017

Chougule, M., Patel, A. R., Sachdeva, P., Jackson, T., & Singh, M. (2011). Anticancer activity of Noscapine, an opioid alkaloid in combination with Cisplatin in human non-small cell lung cancer. *Lung Cancer (Amsterdam, Netherlands)*, *71*(3), 271–282. https://doi.org/10.1016/j.lungcan.2010.06.002

Dahlström, B., Mellstrand, T., Löfdahl, C. G., & Johansson, M. (1982). Pharmacokinetic properties of noscapine. *European Journal of Clinical Pharmacology*, *22*(6), 535–539. https://doi.org/10.1007/BF00609627

Dash, S. G., Suri, C., Nagireddy, P. K. R., Kantevari, S., & Naik, P. K. (2020). Rational design of 9-vinyl-phenyl noscapine as potent tubulin binding anticancer agent and evaluation of the effects of its combination on Docetaxel. *Journal of Biomolecular Structure & Dynamics*, *39*(14), 5276–5289. https://doi.org/10.1080/07391102.2020.1785945

Dash, S. G., Kantevari, S., & Naik, P. K. (2021). Combination regimen of amino-noscapine and docetaxel for evaluation of anticancer activity. *Analytical Chemistry Letters*, *11*(2), 215–229. https://doi.org/10.1080/22297928.2021.1896380

Dash, S. G., Kantevari, S., Guru, S. K., & Naik, P. K. (2021). Combination of docetaxel and newly synthesized 9-Br-trimethoxybenzyl-noscapine improve tubulin binding and enhances antitumor activity in breast cancer cells. *Computers in Biology and Medicine*, *139*, 104996. https://doi.org/10.1016/j.compbiomed.2021.104996

Dash, S. G., Kantevari, S., Pandey, S. K., & Naik, P. K. (2021). Synergistic interaction of N-3-Br-benzyl-noscapine and docetaxel abrogates oncogenic potential of breast cancer cells. *Chemical Biology & Drug Design*, *98*(3), 466–479. https://doi.org/10.1111/cbdd.13902

Dash, S. G., & Naik, P. K. (2022). 9-VINYL PHENYL NOSCAPINE AS POTENTIAL TUBULIN BINDING ANTICANCER AGENT. *Biotechnology*, *39*(14),101–115.

Dash, S. G., Joshi, H. C., & Naik, P. K. (2023). Noscapinoids: A family of microtubule-targeted anticancer agent. In A. N. Grace, P. Sonar, P. Bhardwaj, & A. Chakravorty (Eds.), *Handbook of porous carbon materials. Materials horizons: From nature to nanomaterials*. Springer. https://doi.org/10.1007/978-981-19-7188-4_35

Gordon, M. S., Binkley, J. S., Pople, J. A., Pietro, W. J., & Hehre, W. J. (1982). Self-consistent molecular-orbital methods. 22. Small split valence basis sets for second-row elements. *Journal of the American Chemical Society*, *104*(10), 2797–2803. https://doi.org/10.1021/ja00374a017

Halgren, T. A., Murphy, R. B., Friesner, R. A., Beard, H. S., Frye, L. L., Pollard, W. T., & Banks, J. L. (2004). Glide: A new approach for rapid, accurate docking and scoring. 2. Enrichment factors in database

screening. *Journal of Medicinal Chemistry*, *47*(7), 1750–1759. https://doi.org/10.1021/jm0306430

Hida, T., Kozaki, K., Muramatsu, H., Masuda, A., Shimizu, S., Mitsudomi, T., Sugiura, T., Ogawa, M., & Takahashi, T. (2000). Cyclooxygenase-2 inhibitor induces apoptosis and enhances cytotoxicity of various anticancer agents in non-small cell lung cancer cell lines. *Clinical Cancer Research: An Official Journal of the American Association for Cancer Research*, *6*(5), 2006–2011.

Hida, T., Kozaki, K., Ito, H., Miyaishi, O., Tatematsu, Y., Suzuki, T., Matsuo, K., Sugiura, T., Ogawa, M., Takahashi, T., & Takahashi, T. (2002). Significant growth inhibition of human lung cancer cells both in vitro and in vivo by the combined use of a selective cyclooxygenase 2 inhibitor, JTE-522, and conventional anticancer agents. *Clinical Cancer Research: An Official Journal of the American Association for Cancer Research*, *8*(7), 2443–2447.

Jordan, M. A., & Wilson, L. (2004). Microtubules as a target for anticancer drugs. *Nature Reviews. Cancer*, *4*(4), 253–265. https://doi.org/10.1038/nrc1317

Kavanagh, J. J., & Kudelka, A. P. (1993). Systemic therapy for gynecologic cancer. *Current Opinion in Oncology*, *5*(5), 891–899. https://doi.org/10.1097/00001622-199309000-00019

Ke, Y., Ye, K., Grossniklaus, H. E., Archer, D. R., Joshi, H. C., & Kapp, J. A. (2000). Noscapine inhibits tumor growth with little toxicity to normal tissues or inhibition of immune responses. *Cancer Immunology, Immunotherapy: CII*, *49*(4–5), 217–225. https://doi.org/10.1007/s002620000109

Lee, C., Yang, W., & Parr, R. G. (1988). Development of the Colle-Salvetti correlation-energy formula into a functional of the electron density. *Physical Review. B, Condensed Matter*, *37*(2), 785–789. https://doi.org/10.1103/physrevb.37.785

Mahaddalkar, T., Naik, P. K., Choudhary, S., Manchukonda, N., Kantevari, S., & Lopus, M. (2017). Structural investigations into the binding mode of a novel noscapine analogue, 9-(4-vinylphenyl) noscapine, with tubulin by biochemical analyses and molecular dynamic simulations. *Journal of Biomolecular Structure & Dynamics*, *35*(11), 2475–2484. https://doi.org/10.1080/07391102.2016.1222969

Manchukonda, N. K., Naik, P. K., Santoshi, S., Lopus, M., Joseph, S., Sridhar, B., & Kantevari, S. (2013). Rational design, synthesis, and biological evaluation of third generation α-noscapine analogues as potent tubulin binding anti-cancer agents. *PloS One*, *8*(10), e77970. https://doi.org/10.1371/journal.pone.0077970

Manchukonda, N. K., Naik, P. K., Sridhar, B., & Kantevari, S. (2014). Synthesis and biological evaluation of novel biaryl type α-noscapine congeners. *Bioorganic & Medicinal Chemistry Letters*, *24*(24), 5752–5757. https://doi.org/10.1016/j.bmcl.2014.10.046

Naik, P. K., Santoshi, S., Rai, A., & Joshi, H. C. (2011). Molecular modelling and competition binding study of Br-noscapine and colchicine provide insight into noscapinoid-tubulin binding site. *Journal of Molecular Graphics & Modelling*, *29*(7), 947–955. https://doi.org/10.1016/j.jmgm.2011.03.004

Nawrocki, S. T., Sweeney-Gotsch, B., Takamori, R., & McConkey, D. J. (2004). The proteasome inhibitor bortezomib enhances the activity of docetaxel in orthotopic human pancreatic tumor xenografts. *Molecular Cancer Therapeutics*, *3*(1), 59–70. https://doi.org/10.1158/1535-7163.59.3.1

Najmanovich, R., Kuttner, J., Sobolev, V., & Edelman, M. (2000). Side-chain flexibility in proteins upon ligand binding. *Proteins: Structure, Function, and Genetics*, *39*(3), 261–268. https://doi.org/10.1002/(sici)1097-0134(20000515)39:3 < 261::aid-prot90 > 3.0.co;2-4

Oliva, M. A., Prota, A. E., Rodríguez-Salarichs, J., Bennani, Y. L., Jiménez-Barbero, J., Bargsten, K., Canales, Á., Steinmetz, M. O., & Díaz, J. F. (2020). Structural basis of noscapine activation for tubulin binding. *Journal of Medicinal Chemistry*, *63*(15), 8495–8501. https://doi.org/10.1021/acs.jmedchem.0c00855

Polak, E., & Ribiere, G. (1969). Note sur la convergence de méthodes de directions conjuguées. *Revue française d'informatique et de recherche opérationnelle. Série rouge*, *3*(16), 35–43. https://doi.org/10.1051/m2an/196903R100351

Rowinsky, E. K. (1997). The development and clinical utility of the taxane class of antimicrotubule chemotherapy agents. *Annual Review of Medicine*, *48*, 353–374. https://doi.org/10.1146/annurev.med.48.1.353

Rowinsky, E. K., & Donehower, R. C. (1991). The clinical pharmacology and use of antimicrotubule agents in cancer chemotherapeutics. *Pharmacology & Therapeutics*, *52*(1), 35–84. https://doi.org/10.1016/0163-7258(91)90086-2

Santoshi, S., Manchukonda, N. K., Suri, C., Sharma, M., Sridhar, B., Joseph, S., Lopus, M., Kantevari, S., Baitharu, I., & Naik, P. K. (2015). Rational design of biaryl pharmacophore inserted noscapine derivatives as potent tubulin binding anticancer agents. *Journal of Computer-Aided Molecular Design*, *29*(3), 249–270. https://doi.org/10.1007/s10822-014-9820-5

Tomayko, M. M., & Reynolds, C. P. (1989). Determination of subcutaneous tumor size in athymic (nude) mice. *Cancer Chemotherapy and Pharmacology*, *24*(3), 148–154. https://doi.org/10.1007/BF00300234

Wang, J., Wang, W., Kollman, P. A., & Case, D. A. (2006). Automatic atom type and bond type perception in molecular mechanical calculations. *Journal of Molecular Graphics & Modelling*, *25*(2), 247–260. https://doi.org/10.1016/j.jmgm.2005.12.005

Ye, K., Ke, Y., Keshava, N., Shanks, J., Kapp, J. A., Tekmal, R. R., Petros, J., & Joshi, H. C. (1998). Opium alkaloid noscapine is an antitumor agent that arrests metaphase and induces apoptosis in dividing cells. *Proceedings of the National Academy of Sciences of the United States of America*, *95*(4), 1601–1606. https://doi.org/10.1073/pnas.95.4.1601

Zhou, J., Gupta, K., Aggarwal, S., Aneja, R., Chandra, R., Panda, D., & Joshi, H. C. (2003). Brominated derivatives of noscapine are potent microtubule-interfering agents that perturb mitosis and inhibit cell proliferation. *Molecular Pharmacology*, *63*(4), 799–807. https://doi.org/10.1124/mol.63.4.799